

# SPATIAL AND TEMPORAL MODELING OF THE URBAN GROWTH AND LAND COVER CHANGES USING REMOTE SENSING, SPATIAL INDEXES AND GIS TECHNIQUES IN IRBID CITY, JORDAN

MASHAGBAH, A. F.<sup>1\*</sup> – IBRAHIM, M.<sup>1\*</sup> – AL-FUGARA, A.<sup>2</sup> – ALZABEN, H.<sup>3</sup>

<sup>1</sup>*Department of Geographic Information Systems and Remote Sensing, Institute of Earth and Environmental Sciences, Al Al-Bayt University, Mafraq, Jordan  
(e-mail: majed.ibrahim@aabu.edu.jo)*

<sup>2</sup>*Department of Engineering Survey, Faculty of Engineering, Al Al-Bayt University, Mafraq, Jordan  
(e-mail: akifmohd @aabu.edu.jo)*

<sup>3</sup>*Department of Mechanical Engineering, Faculty of Engineering, Al Hussein Technical University, Amman, Jordan  
(e-mail: heba.alzaben@htu.edu.jo)*

*\*Corresponding authors*

*e-mail: atef.mashagbah@yahoo.com, atef.almashagbah@aabu.edu.jo, majed.ibrahim@aabu.edu.jo; phone: +962-77-678-7720*

(Received 14<sup>th</sup> Jan 2022; accepted 2<sup>nd</sup> May 2022)

**Abstract.** This study examined the temporal and spatial changes in the urban land cover of the northern region of Jordan from 2000 to 2020. Automated processing of satellite images was carried out and different statistical indicators were applied to analyze the data. The data facilitated the monitoring of urban sprawl and determination of trends based on the Geographic Information System (GIS) and remote-sensing analysis of Landsat satellite images. The results revealed an increase in urban segments, population, and reverse migration compared to neighboring areas. The classified land use and land cover maps depicted an expansion of 19.22% from 2000 to 2010 and 8.04% from 2010 to 2020. In comparison to the areas at the urban saturation stage, more rapid urban growth was observed in the seven southwest and northwest districts. Thus, the study presents reliable information and a cartographic database to demonstrate the changes in urban cover of Irbid city, over the past 20 years.

**Keywords:** *land use, spatial and temporal patterns, sprawl, Landsat, urban expansion, Shannon entropy*

## Introduction

Land use maps provide accurate and updated spatial information about the nature of land usage in the target areas. Their applications have become of key importance to plan and develop land resources and achieve maximum benefits for humans (Tewolde and Cabral, 2011). GIS and remote sensing are credible techniques to identify and study land usage. These techniques involve the linking of spatial data to the databases, which is analyzed to identify types and patterns of land usage. The patterns of land use form polygons where each type of land use contains a unit or group of cadastral units indicating industrial, commercial, and residential, areas. These methods provide reliable projections by identifying the empty spaces on the maps for future constructions and the expansion of cities (Eyoh et al., 2012; Kumar et al., 2015).

Urban sprawl is a contemporary global issue, especially in developing countries with higher population-increase rates. This phenomenon of urban sprawling leads to the significant encroachment of agricultural lands, which previously served as the source of

economic activity by producing valuable human foods (Cohen, 2006; Al Mashagbah, 2016; Ibrahim and Al-Mashagbah, 2016; Ibrahim, 2016). Thus, urban sprawl refers to the expansion of cities and suburbs in agricultural and bare land, which transforms rural areas into city margins having high population densities. Urban sprawl is characterized by disorganized, uneven, and unplanned growth that results in unequal distribution of natural resources and services. The area covered by buildings also significantly increases during the urban expansion that decreases agricultural land area leading to reduced food stocks (Habibi, 2011). Multiple environmental problems are also associated with the increased urban constructions such as the lack of arable land, which reduces per-capita agricultural production of fruits and vegetables. The population growth and urban expansion raise the levels of water pollution and consumption, as well as air pollution due to increased traffic burdens. These factors ultimately accumulate to pose serious health concerns for the human population (Ren et al., 2013; Litman, 2020). Several factors such as erosion, human interference, and environmental factors contribute to land cover change. The tools of remote sensing and GIS techniques can effectively detect these changes by generating accurate reports and maps (Barkhordari, 2003; Ibrahim and Al-Mashagbah, 2016). The application of these systems becomes more crucial in areas under continuous urban development. These scientific and analytical tools facilitate the optimal utilization of available resources. Based on the generated information, the available resource could be managed accordingly to achieve the maximum output, which contributes towards a balanced and functional urban system through an easy and efficient decision-making process. Higher population growth rates leading to increased housing demands are the main factor affecting agricultural lands through urban sprawl. The constructions of roads for transportation, urban infrastructure, and factories near roads also result in the urbanization of agricultural lands (Zhao et al., 2006; Rawat and Puri, 2017). The recent increase in the Jordanian population is associated with the urbanization of either cultivated agricultural lands or lands under natural vegetation. The removal of vegetation cover over large areas has disturbed the ecological balance and reduced agricultural production. This study employed remote sensing, GIS, and statistical indicators to analyze the urban sprawl of the Irbid city and highlights the factors, which transformed its agricultural lands into residential areas.

## Materials and methods

### *Study area*

The selected area is Irbid city which is located in the northern region of Jordan, 71 km north of the capital city of Amman, and 15 km south of the Syrian-Jordanian border. It is in the central part of the Irbid Governorate within the Horan plain area. Population wise, Irbid is the third-largest city in the Kingdom of Jordan after the capital city of Amman and Zarqa. According to the recent census of 2017, the population of Irbid and its suburbs was over 530,200 (Norway, 2008). Irbid is an important industrial city of Jordan which, along with its population density and geographical location have made it a large commercial area. The study area extends between latitudes 32° 31' 15" and 32° 35' 33" north and longitudes 35° 48' 00" and 35° 53' 00 East, covering a total of 36.86 km<sup>2</sup> across seven residential districts of varying size (Barha, Hashimiyah, Manara, Naser, Nozha, Rabea, and Rabea) as presented in *Figure 1*.

The altitude of the study area ranges between 324 m above sea level in the northwest and 677 m above sea level in the southwest districts. The climate of Irbid city significantly

fluctuates between summer and winter, especially in areas well above the sea level. The city receives significant rainfall during winter and snowfalls in the high-altitude areas. The city and its surrounding areas are famous for soil fertility, being part of the Horan plains, where multiple field crops, grains, and fruit trees (especially olive trees) are grown.

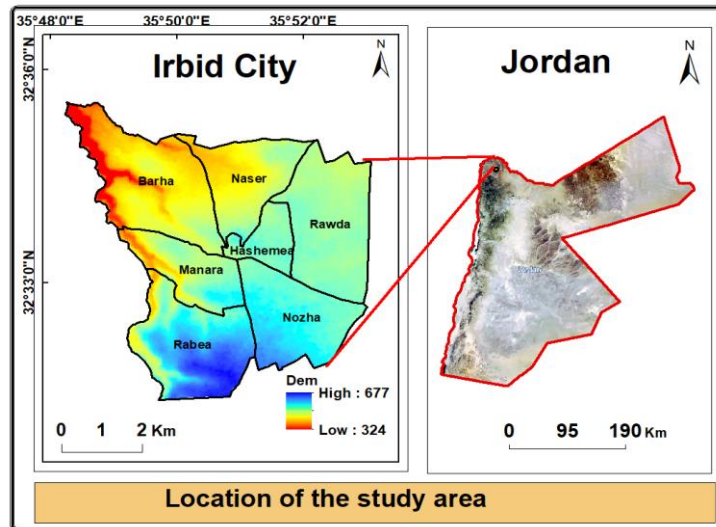


*Figure 1. The location of Irbid city districts*

### ***Data collection***

Three Landsat images with a cloud cover of less than 10% were selected to avoid classification errors, which were defined for path 174 and row 37 covering Irbid city. The first and second images from the Landsat-7 Enhanced Thematic Mapper Plus were captured on July 8, 2000, and September 6, 2010, respectively. The third image was obtained on August 24, 2020, using Landsat-8 Operational Land Imager. All images were downloaded from the USGS website (<https://earthexplorer.usgs.gov/>).

### ***Image processing***

Initially, before subjecting the images to classification, image pre-processing was carried out through image enhancement, geometric correction, and visual interpretation to make the images are more interpretable to human eye. The geometric correction process adjusted the distortion to produce a corrected image in the correct geographic location. The Landsat images were thus geo-referenced to UTM WGS 1984 Zone 36N using distinguishable points such as intersections, roads, and corners as seen on Google Earth maps, rectified digital topographical map, and a reference shapefile of the study area. All systematic errors and radiometric corrections were removed from the Landsat data, even though the land cover maps can be classified without performing any radiometric or atmospheric corrections (Kamal et al., 2020). The satellite images were reduced to a subset, covering Irbid city and a surrounding area of about 36.86 km<sup>2</sup>. All bands of each satellite image were stacked into a single file to form an RGB multiband and a multi-color composite Tiff layer.

The digital classification technique divides the cells of the multi-spectral image into classes based on their spectral signature, which represents the reflectivity of the land

cover in the spectral reflectance. Supervised and unsupervised classification techniques are used for satellite image classification through remote sensing. The unsupervised classification technique is purely statistical and does not require training data for the classification. Contrarily, the supervised classification requires user-defined training data from the field or high-resolution maps (Google Earth) before carrying out the classification process. A maximum likelihood supervised classification method is more accurate than the unsupervised classification method (Currit, 2005; Hasmadi et al., 2005; Ahmad and Quegan, 2013). This study aimed to extract satellite images based-classification of land use in Irbid city, therefore, a maximum likelihood supervised classification tool in ArcMap software was used. The three classified images were divided into two classes, (urban and non-urban land) to investigate temporal and spatial changes in the land use of the study area. The differences between the images were identified as natural or man-made changes between 2000 and 2020. The classified images were converted from raster to vector format using ArcGIS software to simplify the calculation of the area of each land-use class. The accuracy of classified maps was verified by generating 100 random samples for each image using ArcMap software. These points were compared with the equivalent Google Earth reference map through field surveys and a GPS device to evaluate the accuracy of classified images. An error matrix was produced for each classified image to calculate the overall accuracy and the Kappa coefficient.

### ***Urban expansion intensity index***

The urban expansion intensity index quantitatively analyses the ongoing differences in the spatial extension of an area. This method determines the tendency of urban growth over a particular period and projects potential future trends of urban expansion. It also compares the speed and intensity of changes in urban land use between different periods. (Zhao-ling et al., 2007), This index was divided as slow growth from 0 to 0.28 (Zhao et al., 2006), low-speed expansion from 0.28 to 0.59, medium-speed expansion from 0.59 to 1.05, high-speed expansion from 1.05 to 1.92, and very high-speed expansion at values greater than 1.92. The urban expansion intensity index of each period and direction was calculated as follows (*Eq. 1*).

$$UI = \frac{\Delta U}{\Delta T \cdot TA} * 100 \quad (\text{Eq.1})$$

where: UI is the urban expansion intensity index of the *i*th zone;  $\Delta U$  is the difference between the urban area of the *i*th zone at time1 and time2; TA is the total land area of the *i*th zone; and  $\Delta t$  is time2-time1.

### ***Pearson's chi-square and urban growth***

A comparative analysis was conducted between observed, theoretical, or expected values of urban expansion in the study area. The expected growth of the urban area was calculated using *Equation 2*.

$$M_{ji} = \frac{M_j \times M_i}{M_g} \quad (\text{Eq.2})$$

where  $M_{ji}$  is the expected growth,  $M_j$  is the column total,  $M_i$  is the row total, and  $M_g$  is the grand total.

The chi-square calculation determined the degree of freedom for urban growth in the study area in different directions at different periods. The degree of freedom indicates the sustainability or unsustainability of the urban growth, whereas a high degree of freedom represents an unbalanced regional process of urban growth (Ren et al., 2013). The degrees of freedom for the entire study area and each direction were calculated using Equation 3 (Ren et al., 2013):

$$X^2 = \sum_{i=1}^n \frac{(O_i - E_i)^2}{E_i} \quad (\text{Eq.3})$$

where  $X^2$  is the overall degree of freedom,  $O_i$  is the observed growth, and  $E_i$  is the expected growth.

### ***Shannon's entropy index***

The measures of contrast cannot be used for categorical data, as median or mean are not available for such data. However, Shannon's entropy index can be used for a random sample of data (Eq. 4). Shannon's index of diversity could calculate and compare biodiversity across communities to represent that how a geographic feature is distributed across a specific area (Kumar et al., 2020; Al Mashagbah, 2016; Wondrade et al., 2014).

$$H_n = \sum_{i=1}^n P_i * \ln(P_i) \quad (\text{Eq.4})$$

Given  $P_i = X_i / \sum_{i=1}^n X_i$ ; where  $n$  is the number of observations and  $P_i$  is the proportion of observations in the  $i$ th of  $n$  categories. The maximum value of entropy occurs when all proportions of observations are equal; as the sum of the  $p_i$  is equal to  $\sum_{i=1}^n P_i = k P_i = 1$ . In addition,  $H_{max} = \ln(n)$ , and the Relative entropy =  $H_n / \ln(n)$ .

### ***Annual urban expansion rate and average annual expansion***

The annual urban expansion rate (AER) shows the relative dynamic change rate of urban expansion among different districts over the same period (Eq. 5), whereas the average annual expansion (AE) quantifies the overtime changes of urban areas and compares the urban growth of the same district over various periods. Following equations (Eqs. 5 and 6) were used for the calculation of these two indexes:

$$\text{AER} = ((LU_j - LU_i) / LU_i) \times (1 / (\Delta t)) \times 100 \quad (\text{Eq.5})$$

$$\text{AE} = (LU_j - LU_i) / \Delta t \quad (\text{Eq.6})$$

where  $LU_i$  and  $LU_j$  represent the urban area at the initial and end period, respectively, whereas  $\Delta t$  represents the change in time.

## **Results**

### ***Urban growth and Pearson's chi-square statistics***

The urban growth rate of each district was calculated from 2000-2010 and 2020-2020 (Table 1). The results demonstrated an overall declining trend in percentage

growth rate except for the Manara district. Higher urban and residential saturation levels could justify this phenomenon. The lowest (0.11%) and the highest (46.36%) growth rates were observed in Hashimiyah and Rabea districts, respectively. Equation 3 was followed to calculate Pearson's chi-square statistics for each temporal interval, and the degree of freedom for each district. The expected growth and the observed growth are considered closely related at a value near zero whereas they are considered significantly diverged at a higher chi-square value. The results reveal a balanced and sustainable urban growth of the study area between 2000 and 2020. A higher degree of freedom represents unbalanced urban growth at different intervals and places within the same area (Ren et al., 2013). The overall degree of freedom of the complete study area remained as 1.14 whereas lower degrees of freedom (0.38 and 0.76) at both temporal intervals (2000-2010 and 2010-2020) revealed a low variation between the expected and observed urban growth. A significantly low degree of freedom (less than 1) in all the districts indicates a higher similarity between expected and observed urban growth and expresses a coherent and balanced urban expansion. The degree of freedom values for Barha, Hashimiyah, Manara, Naser, Nozha, Rabea, and Rawda districts were noted as 0.17, 0.00, 0.08, 0.15, 0.04, 0.18, and 0.52, respectively. The highest degree of freedom (0.52) was recorded in the Rawda district, whereas the lowest (almost zero) value was observed for the Hashimiyah district.

**Table 1.** Urban growth rates

Period	Barha	Hashimiyah	Manara	Naser	Nozha	Rabea	Rawda	Total area
2010-2000	29.0%	0.2%	3.8%	15.8%	13.8%	46.4%	23.9%	19.2%
2020-2010	20.6%	0.1%	5.3%	1.6%	3.7%	28.9%	0.8%	8.0%

### Shannon's entropy

Shannon's entropy analysis of different districts of Irbid city demonstrated a disparity among the urban areas of each district. The entropy values reflected the variations based on the area and density of urbanization in each district. Table 2 presents the collective entropy values of all the districts at two intervals (2000-2010 and 2010-2020) whereas Table 3 separately depicts the values of each district. The entropy values from 2000 to 2010 (1.61) and 2010 to 2020 (1.26) indicate the differences in the urban growth patterns for the specified years. These entropy values (1.95) were calculated to be greater than half of  $\ln(n)$  representing that the Irbid city sprawled during the complete study period. However, the decreased entropy value during the second period (2010-2020) suggests that the city became more compact, especially in certain districts. In terms of individual districts, Shannon's entropy value for the Rawda district showed a lower degree of dispersion for build-up that indicates a higher urban density or more compact urban growth. The Barha and the Manara districts showed higher dispersion (close to  $\ln(n)$  (0.69)), thus indicating more dispersed distribution in these districts.

**Table 2.** Shannon's entropy for both periods ( $n = 7$ )

Time period	Entropy	Log (n)	1/2 Log(4)
2000-2010	1.61	1.95	0.97
2010-2020	1.26	1.95	0.97

**Table 3.** Shannon's entropy for the different districts ( $n = \text{sum of both interval} = 2$ )

District	Barha	Hashimiyah	Manara	Naser	Nozha	Rabea	Rawda
Entropy	0.68	0.64	0.68	0.31	0.52	0.67	0.14
Log (n)	0.69	0.69	0.69	0.69	0.69	0.69	0.69

### Intensity of urban expansion and rate of expansion

The intensity index was used to standardize the average of the annual expansion speeds of different districts at different times (Jianhua et al., 2003). Urban expansion intensity declined from 1.23 (2000-2010) to 0.61 (2010-2020). According to Zhao-ling et al. (2007), the first period displays high-speed urban expansion followed by medium-speed expansion during the second period that implies a decrease in urban sprawl (Table 4).

**Table 4.** Area of expansion, urban expansion rate, and expansion intensity in Irbid City from 2000 to 2020

Period	Area of expansion km <sup>2</sup> /y	Expansion rate %	Expansion intensity %
2000-2010	0.45	1.92	1.23
2010-2020	0.23	0.80	0.61
2000-2020	0.34	1.44	0.92

The intensity of urban expansion in the seven urban districts is presented in Figure 2. The highest urban expansion intensity (0.34) was noted for Rawda district from 2000 to 2010 whereas the lowest value was observed for the Hashimiyah district because it had already reached its urban saturation point. However, a decline in urban expansion intensity during both periods was noticed in most of the districts.

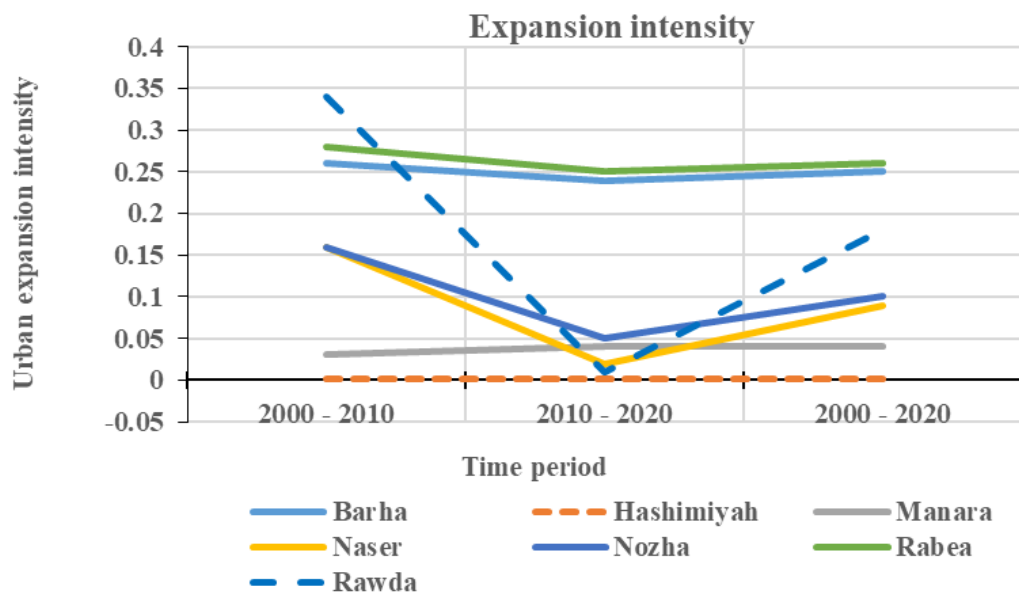


**Figure 2.** Urban expansion intensities of the seven districts

The urban area collectively expanded from 23.6 km<sup>2</sup> in 2000 to 30.39 km<sup>2</sup> in 2020 at a rate of 0.34 km<sup>2</sup>/year over the last two decades. The expansion in the urban land area was continuous even though the intensity of expansion comparatively decreased in the second period (2010-2020). The urban areas expanded by 4.53 km<sup>2</sup>/year from 2000 to 2010 and decreased to 2.6 km<sup>2</sup>/year from 2010 to 2020. The complete study area expanded at a rate of 0.45 km<sup>2</sup>/year (1.92%) from 2000 to 2010 and at a relatively lower expansion rate of 0.23 km<sup>2</sup>/year (0.8%) from 2010-2020. The highest expansion rates occurred in the southwest Rabea district (4.43%) and northeast Barha district (2.77%) from 2000 to 2020. Contrarily, the lowest expansion rates of 0.02% and 0.47% were noted for central Hashimiyah and Manara districts, with lower expansion intensities of 0.001% and 0.4%, respectively, due to urban saturation. Northwest and Southwest directions exhibited the highest urbanization trend as these areas are near to the already saturated.

## Discussion

### *Land use/land cover change*

Human activities lead to significant changes in land use. These land-use changes are detected by figuring out the changing class in comparison to others at a given time (Zubair, 2006; Pandey and Nathawat, 2006). The open-source U.S. Landsat data (ETM + and OLI) was utilized in this study to classify the land use and land cover. Satellite images with a 30 m spatial resolution captured in 2000, 2010, and 2020 were classified by following the supervised classification method in ArcMap 10.4 to detect and determine different classes of land in the study area. Two classes of land use (urban and non-urban) were selected based on the visual interpretations of the satellite images, Google Earth maps, field observations, and previous reports of land cover and land use of the study area. Urban areas consist of built-up areas including roads, commercial or industrial areas, and residential areas. The drylands, agricultural lands, uncultivated lands, and green spaces (irrigated vegetable crops, forests, or fruit trees) represent non-urban areas. The accuracy of classified maps was validated by creating a set of 100 random points in ArcMap software that were distributed across each image. These points were converted to KML format to open in Google Earth for verification with high-resolution Google images. Confusion matrices were generated for all classified images to calculate the Kappa coefficient and the overall accuracy between each classified map and reference data. The overall accuracy of classification images captured in 2000, 2010, and 2020 was calculated as 93%, 93%, and 94%, respectively. Simultaneously, the Kappa coefficient of 2000, 2010, and 2020 satellite images was estimated as 83.2%, 82.4%, and 84%, respectively. These values are in the acceptable range. According to Congalton and Green (2019), a Kappa value of 60% to 80% represents substantial agreement whereas greater than 80% indicates strong agreement between classified map and reference data. Similarly, a value of more than 0.75 indicates “a very good to an excellent” agreement according to (Monserud and Leemans, 1992). A continuous increasing trend of urban land cover was observed during the study period that accounted for 63.99%, 76.29%, and 82.42% of the land areas in 2000, 2010, and 2020, respectively. The proportion of bare and agricultural land reduced over time in contrast to urban areas. The land cover and land use maps indicated a significant increase in the urban areas at the expense of agricultural and bare lands. The main reasons for unregulated urban sprawl include the



rising population during the past 20 years, the reverse migration from villages close to the city, and Syrian refugees. There was an increase of about 4.53 km<sup>2</sup> (19.22%) of the urban area during the first decade (2000-2010) whereas it increased by 2.26 km<sup>2</sup> (8.04%) from 2000-2010. The total increase in the urban area in bare and agricultural lands from 2000 to 2020 was estimated as 22.36%. The annual increase rate of urban areas in Irbid was calculated as 0.45 km<sup>2</sup>/year from 2000 to 2010 and 0.23 km<sup>2</sup>/year from 2010 to 2020. A higher urban saturation in Nozha (92.7%), Rawda (94.5%), Naser (97.8%), and Hashimiyah (99%) districts led to the decrease in urban expansion during the second decade (2010-2020). The economic development and increasing demographic pressure in the city center have urged the residents to move to the agricultural and bare lands of city surroundings. This phenomenon has resulted in increased residential areas in the city outskirts and the transformation is ultimately declining the agricultural and barren land areas. The Syrian civil war also led to a major migration of Syrian refugees to Jordan after 2010, especially to the northern governorates of Irbid and Mafraq that also contributed to an increase in the urban areas. The immigration from neighboring villages to Irbid for economic activities has also had an impact. The data analysis revealed that the urban area increased in all districts during the study period (2000-2020). Overall, the urban area increased from 23.60 km<sup>2</sup> in 2000 to 30.39 km<sup>2</sup> in 2020. The Population and commercial growth of the city has resulted in the rapid increase in industrial, residential, and commercial areas, and necessary infrastructure networks. The Rabea district, being the commercial and service center of the city, exhibited the highest level of urban growth. This area is near Yarmouk University and other buildable spaces. Urban sprawl is also quite significant in the Rabea, Barha, and Rawda districts as they have sufficient space for industrial, residential, and commercial growth. The land prices are also comparatively lower in these areas as compared to the areas near the city center. The significant expansion in the urban areas of various residential districts is presented in *Figure 3* from the years of 2000 to 2010 and years of 2010 to 2020. The results depict that the built-up areas expanded significantly in the Rabea, Barha, and Rawda districts, and at a comparatively lower rate in the Naser district. Contrarily, a horizontal expansion in the Manara and the Hashimiyah districts has now almost ceased due to the limited space and lack of construction land. Generally, only a minimal variation was observed among the growth patterns of urban sprawl and its trends in different districts. Horizontal urban sprawl has consumed some of the most fertile agricultural lands in several provinces and developing urban areas at the expense of olive and grape plantations, and wheat and barley fields are dangerous. The Rawda, Barha, and Nozha districts exhibited the highest expansion of urban area whereas the rate of urban expansion was noted to be lowest in Hashimiyah and Manara districts. The proportion of urban area in Rabea and Barha districts was less than 50% in 2000 in comparison to other districts. However, only the Rabea district had less than 50% area in 2010 whereas all other districts had more than 50% urban area by 2020. The urban areas of Hashimiyah, Naser, Nozha, and Rawda districts have reached up to more than 90% of their total areas. The urban growth was noted in all districts from 2000 to 2020, which can be attributed to population growth, and migration from the countryside to the city for jobs and accessing various services. Rabea and Barha districts proportionally showed the highest increase in the urban area during the study period as their urban land use grew from less than 50% in 2000 and 2010, to well over that in 2020. Hashimiyah and Manara districts demonstrated the lowest expansion of urban areas

during the same period. During the second decade (2010 to 2020), urban areas rapidly increased in Rabea and Barha districts, whereas vertical construction mostly occurred in the Hashimiyah district leading to the least horizontal expansion of the urban area.

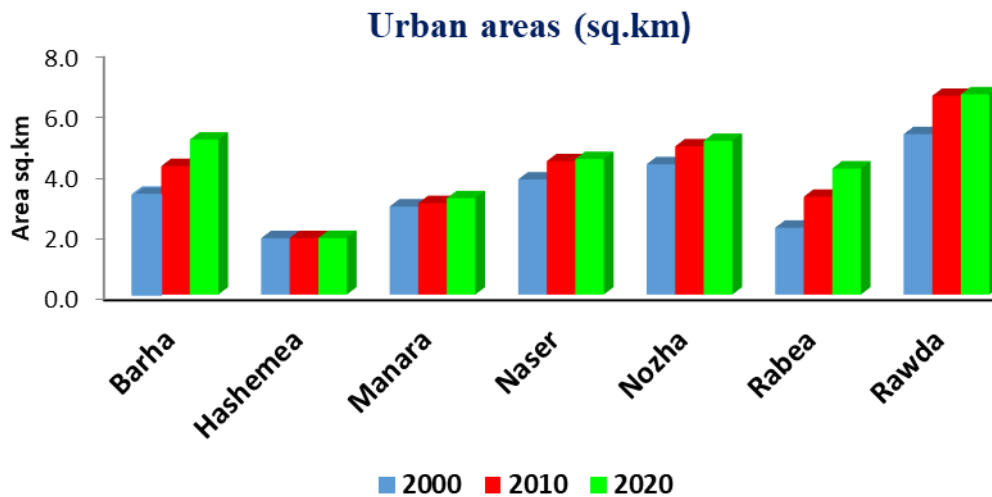


Figure 3. Urban areas (km<sup>2</sup>) included in the study

According to the data of 2020, almost 88%, 93%, 95%, 98%, and 99% of the land in Manara, Nozha, Rawda, Naser, and Hashimiyah districts, respectively, could be considered urban. The lowest percentages of urban areas were noted in Rabea (63%) and Barha (65%) districts. Generally, 64%, 76.3%, and 82.4% of the overall land in 2000, 2010, and 2020, respectively, was residential and urban land, which increased by 19.22% from 2000 to 2010, and 8.04% from 2010 to 2020. The slowdown of urban growth during the second decade could be mainly attributed to the urban saturation in most of the districts within the city. Two main classes were extracted based on the data as shown in Figure 4.

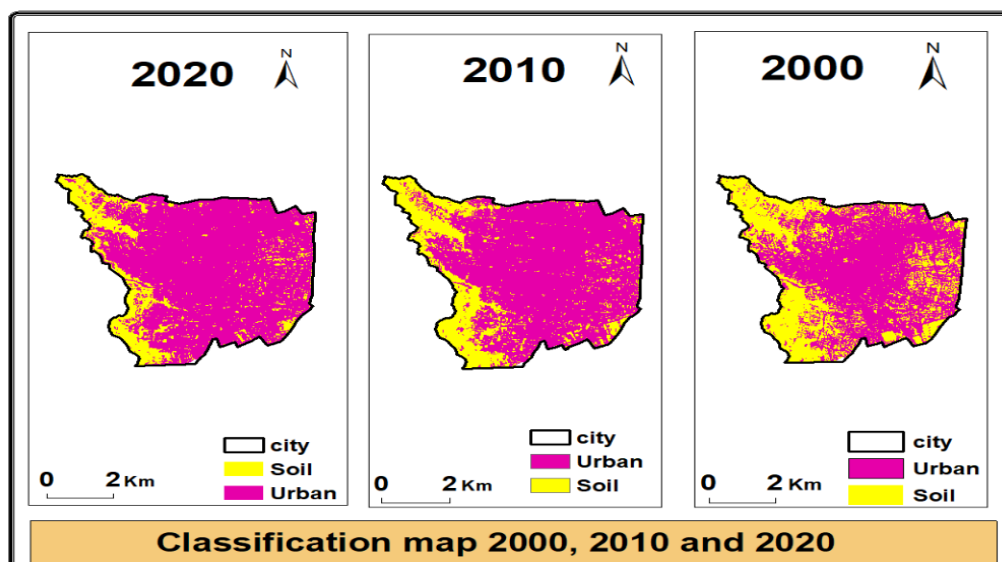


Figure 4. Classified images of three periods depicting urban and non-urban lands

## Conclusions

The study efficiently determined the land cover changes in Irbid city from the period of 2000 to 2020 by employing GIS and remote sensing techniques combined with different statistical indicators. The results revealed the effectiveness of GIS and remote-sensing techniques to produce accurate maps describing different types of land use. The Landsat satellite images were classified into two main classes of urban land and nonurban land. A map was extracted for the specific years of interest, and areas were calculated to compare the changes over time. A significant increase in urban areas corresponding to a decrease in the percentage of non-urban lands was observed in 2010 and 2020 as compared to the year 2000. The urban sprawl occurred by utilizing precious barren and agricultural lands, which could affect the agricultural produce in the future. The increase in urban lands and the decline of green lands may lead to some environmental problems such as increasing pollution; also the rapid urban growth may poses a serious burden on electricity, sewage, water, and transportation systems. However, the government has taken effective measures by establishing infrastructures in residential, industrial, agricultural, and commercial lands for the smooth conversion of lands into urban areas. This study will further facilitate the development of effective policies for managing urban sprawl in the future.

The use of geographic information systems requires effort, accuracy, and cost and gives accurate and fast results, and it can conduct spatial and attribute data analysis. The application of GIS, which provides the possibility of handling, processing, and analyzing a large volume of data, helps to increase the efficiency of land use studies; therefore, we recommend a similar and continuous future studies on the study area and on other similar areas to monitor urban development and its impact on the deterioration of agricultural land.

**Funding.** This research received no external funding.

**Conflict of interests.** The authors declare no conflict of interests.

## REFERENCES

- [1] Ahmad, A., Quegan, S. (2013): Comparative analysis of supervised and unsupervised classification on multispectral data. – *Applied Mathematical Sciences* 7(74): 3681-3694.
- [2] Al Mashagbah, A. F. (2016): The use of GIS, remote sensing and Shannon's entropy statistical techniques to analyze and monitor the spatial and temporal patterns of urbanization and sprawl in Zarqa City, Jordan. – *Journal of Geographic Information System* 8(2): 293-300.
- [3] Barkhordari, J. (2003): Assessing the effects of land use change on the hydrologic regime by RS and GIS. Assessing the effects of land use change on the hydrologic regime by RS and GIS. – Thesis, International Institute for Geo-Information Science and Earth Observation, Enschede.
- [4] Cohen, B. (2006): Urbanization in developing countries: current trends, future projections, and key challenges for sustainability. – *Technology in Society* 28(1-2): 63-80.
- [5] Currit, N. (2005): Development of a remotely sensed, historical land-cover change database for rural Chihuahua, Mexico. – *International Journal of Applied Earth Observation and Geoinformation* 7(3): 232-247.

- [6] Eyoh, A., Olayinka, D. N., Nwilo, P., Okwuashi, O., Isong, M., Udoudo, D. (2012): Modelling and predicting future urban expansion of Lagos, Nigeria from remote sensing data using logistic regression and GIS. – *International Journal of Applied Science* 2(5): 1-9.
- [7] Habibi, S., Asadi, N. (2011): Causes, results and methods of controlling urban sprawl. – *Procedia Engineering* 21: 133-141.
- [8] Hasmadi, M., Pakhriazad, H. Z., Shahrin, M. F. (2005): Evaluating supervised and unsupervised techniques for land cover mapping using remote sensing data. – *Geografia-Malaysian Journal of Society and Space* 5(1): 1-10.
- [9] Ibrahim, M. M. (2014): The use of geoinformatics in investigating the impact of agricultural activities between 1990 and 2010 on land degradation in NE of Jordan. – PhD Dissertation, Faculty of Environmental and Natural Sciences, Freiburg University, Freiburg im Breisgau.
- [10] Ibrahim, M. (2016): Temporal interpretation for land use/land cover changes using multispectral images: Irbid as a case study. – *Journal of Natural Sciences Research* 6(5): 100-104.
- [11] Ibrahim, M., Al-Mashagbah, A. (2016): Change detection of vegetation cover using remote sensing data as a case study: Ajloun area. – *Civil and Environmental Research* 8(5).
- [12] Jianhua, X., Changlin, F., Wenze, Y. (2003): An analysis of the mosaic structure of regional landscape using GIS and remote sensing. – *Acta Ecologica Sinica* 23(2): 365-75.
- [13] Kamal, M., Muhammad, F. H., Mahardhika, S. A. (2020): Effect of image radiometric correction levels of Landsat images to the land cover maps resulted from maximum likelihood classification. – *International Conference on Sustainability Science and Management: Advanced Technology in Environmental Research (CORECT-IJSS 2019)*. <https://doi.org/10.1051/e3sconf/202015302004>.
- [14] Kumar, K. S., Valasala, N. V., Subrahmanyam, J. V., Mallampati, M., Shaik, K., Ekkirala, P. (2015): Prediction of future land use land cover changes of Vijayawada city using remote sensing and GIS. – *International Journal of Innovative Research in Advanced Engineering* 2(3): 91-97.
- [15] Litman, T. (2016): Determining optimal urban expansion, population and vehicle density, and housing types for rapidly growing cities. – *World Conference on Transport Research - WCTR 2016 Shanghai, 10-15 July 2016*.
- [16] Monserud, R. A., Leemans, R. (1992): Comparing global vegetation maps with the Kappa statistic. – *Ecological Modelling* 62(4): 275-93.
- [17] Norway, S. (2008): Population and housing census. Population and housing census. <https://www.ssb.no/en/befolkning>
- [18] Pandey, A. C., Nathawat, M. (2006): Land use land cover mapping through digital image processing of satellite data. A case study from Panchkula Ambala and Yamunanagar districts, Haryana State, India. – *Geospatial World*.
- [19] Rawat, V., Puri, M. (2017): Land use/land cover change study of district Dehradun, Uttarakhand using Remote sensing and GIS technologies. – *International Journal of Advanced Remote Sensing and GIS* 6(1): 2223-2233.
- [20] Ren, P., Gan, S., Yuan, X., Zong, H., Xie, X. (2013): Spatial Expansion and Sprawl Quantitative Analysis of Mountain City Built-up Area. – In: Bian, F. et al. (eds.) *Geoinformatics in Resource Management and Sustainable Ecosystem*. International Symposium, GRMSE 2013, Wuhan, China, November 8-10, 2013, Proceedings, Part II. Springer, Berlin, Heidelberg, pp. 166-176.
- [21] Tewolde, M. G., Cabral, P. (2011): Urban sprawl analysis and modeling in Asmara. – *Remote Sensing* 3(10): 2148-2165.
- [22] Wondrade, N., Dick, O. B., Tveite, H. (2014): Landscape mapping to quantify degree-of-freedom, degree-of-sprawl, and degree-of-goodness of urban growth in Hawassa, Ethiopia. – *Environment and Natural Resources* 4(4): 223-237.

- [23] Zhao, S., Da, L., Tang, Z., Fang, H., Song, K., Fang, J. (2006): Ecological consequences of rapid urban expansion: Shanghai, China. – *Frontiers in Ecology and the Environment* 4(7): 341-346.
- [24] Zubair, A. O. (2006): Change Detection in Land Use and Land Cover Using Remote Sensing Data and GIS (A Case Study of Ilorin and Its Environs in Kwara State). – Department of Geography, University of Ibadan, Nigeria.